ChemComm

COMMUNICATION

View Article Online
View Journal | View Issue

Cite this: *Chem. Commun.*, 2021, **57**, 5406

Received 17th March 2021,
Accepted 29th April 2021

DOI: 10.1039/d1cc01441b

rsc.li/chemcomm

Chiral metal down to 4.2 K - a BDH-TTP radical-cation salt with spiroboronate anion B(2-chloromandelate)$_2^-$†

Toby J. Blundell, [a] Michael Brannan,[a] Hiroshi Nishimoto, [b] Tomofumi Kadoya, [b] Jun-ichi Yamada,[b] Hiroki Akutsu, [c] Yasuhiro Nakazawa[c] and Lee Martin *[a]

We report the first example of a chiral BDH-TTP radical-cation salt. Chirality is induced in the structure *via* the use of a chiral spiroborate anion where three stereocentres are present, one on each chiral ligand and one on the boron centre. Despite starting from a labile racemic mixture of B_S and B_R enantiomers, only one enantiomer is present in the crystal lattice. The anions pack in a novel double anion layer which is the thickest anion layer found in a BDH-TTP salt. This material is chiral and shows metallic behaviour down to at least 4.2 K.

The combination of conductivity and chirality in the same material is not found in nature and the inclusion of chirality in conducting materials has been a hotly pursued topic since the discovery of electrical magneto-chiral anisotropy (eMChA).[1] Differences in resistivity in applied magnetic fields have since been observed for chiral enantiomers of bismuth helices[1] and carbon nanotubes.[2] Non-reciprocal charge transport has also recently been observed in non-centrosymmetric superconductors such as WS_2 nanotubes and MoS_2 thin single crystals.[3] However, the chiral nature of these inorganic materials cannot be controlled because they happen to crystallise in non-centrosymmetric structures. Molecular materials containing stereogenic centres on the other hand can be synthesised in both enantiomeric forms and also the racemate to allow a study of their physical properties in each form. As such, there is a huge interest in the synthesis of molecular chiral conducting materials.[4]

The first bulk conductor to exhibit eMChA was reported in 2014 by Pop and co-workers.[5] A pair of enantiopure radical-cation salts of dimethyl-ethylenedithio-tetrathiafulvalene (DM-EDT-TTF) with ClO_4^- anions were crystallised in the space groups $P6_222$ and $P6_422$ and showed metallic behaviour down to 40 K. Chiral molecular conductors provide an excellent opportunity to study eMChA and there are several sources to introduce chirality into radical-cation salts: *via* chiral donors,[6] chiral anions[7] or chiral solvents.[8]

The use of chiral spiroboronate anions in radical-cation salts allows the introduction of multiple chiral centres on the same anion, and we have previously reported that this can result in chiral crystallisation where only specific enantiomers crystallise in the radical-cation salt despite a racemic anion mixture being present in solution.[9]

The most successful method for producing chiral radical-cation salts has been by means of enantiopure donors based on EDT-TTF[10] or BEDT-TTF.[11] Whilst still difficult to obtain highly crystalline materials, the donor tetramethyl-BEDT-TTF has produced several enantiopure salts.[12] As an alternative to BEDT-TTF, we have utilised the donor 2,5-bis(1,3-dithiolan-2-ylidene)-1,3,4,6-tetrathiapentalene (BDH-TTP) which has a tendency to form a κ-type packing arrangement and show metallic behaviour.[13]

We report the first enantiopure radical-cation salt of BDH-TTP, κ-BDH-TTP$_2$[B_S-(*S*-ClMan)$_2$] (ClMan = 2-(2-chlorophenyl)-2-oxidoacetate) **I** which crystallises in the $P2_1$ space group where the asymmetric unit contains two crystallographically independent BDH-TTP molecules and one [B_S(*S*-ClMan)$_2$]$^-$ anion, with no other guest or solvent molecules being present (Fig. 1).‡

The crystal lattice of the salt contains alternating layers of κ-type packed BDH-TTP and anionic layers containing the enantiopure [B_S(*S*-ClMan)$_2$]$^-$ anion. The anion contains three stereocentres with two enantiopure *S*-chloromandelate ligands bound to a boron centre *via* oxygens, resulting in tetrahedral coordination, and the introduction of a chiral centre at boron (Fig. 2).

Salt **I** shows the presence of only a single enantiomer at boron (B_S) despite the electrocrystallisation experiment starting

[a] *School of Science and Technology, Nottingham Trent University, Clifton Lane, Nottingham, NG11 8NS, UK. E-mail: lee.martin@ntu.ac.uk*
[b] *Graduate School of Material Science, University of Hyogo, Kamigori-cho, Ako-gun, Hyogo, 678-1297, Japan*
[c] *Department of Chemistry, Graduate School of Science, Osaka University, 1-1 Machikaneyama, Toyonaka, Osaka 560-0043, Japan*

† Electronic supplementary information (ESI) available: Fig. S1–S3 and Tables S1, S2. CCDC 2069593. For ESI and crystallographic data in CIF or other electronic format see DOI: 10.1039/d1cc01441b

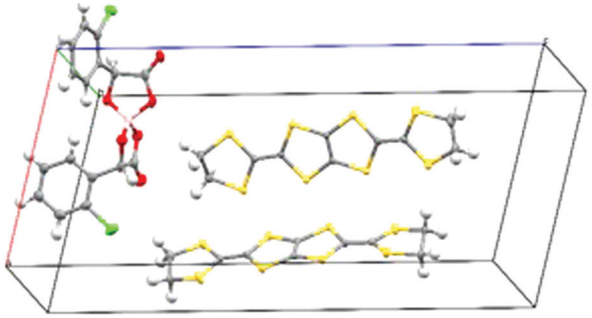

Fig. 1 Asymmetric unit cell for **I**.

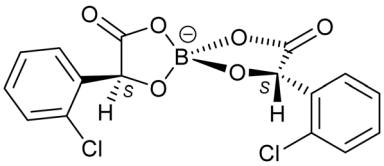

Fig. 2 Single enantiomer of B_S(*S*-chloromandelate)$_2$.

from a labile racemic mixture of B_S and B_R enantiomers of the anion. We have observed this chiral selectivity in previous examples where a racemic mixture of spiroboronate anions is present in solution but a single enantiomer is preferentially crystallised during crystal growth.[9] Wong *et al.* have reported differences in shape for the twisted B_R- and the V-shaped B_S-$[(S\text{-Man})_2]^-$ anions leading to preferential packing and crystallisation with various cations in their resolution studies.[14] The spiroboronate forms a double anion layer, as can be seen in Fig. 3 and 4, in contrast to previous κ-type BDH-TTP salts which have a single layer of anions.[13] This results in an anion layer considerably thicker than for other BDH-TTP salts with the distance between terminal ethylene moieties of adjacent BDH-TTP layers of 10.246 Å.

The donor layer of salt **I** contains two crystallographically independent BDH-TTP molecules (shown in red and blue in Fig. 5) which dimerise face-to-face along the *ab* crystallographic axis. Dimers stack in the so-called ''chess-board'' pattern perpendicular to each other resulting in a κ-type arrangement. In this arrangement, a pair of donors are arranged parallel to each other whilst neighbouring donor pairs are arranged perpendicular to the parallel pair (Fig. 5).

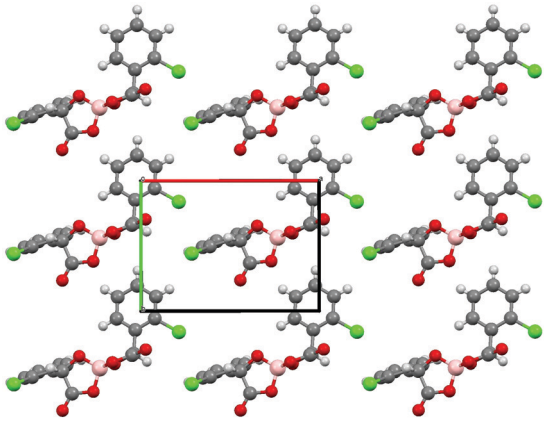

Fig. 3 Packing of single enantiomer of B_S(*S*-chloromandelate)$_2$ in a single anion layer of **I**.

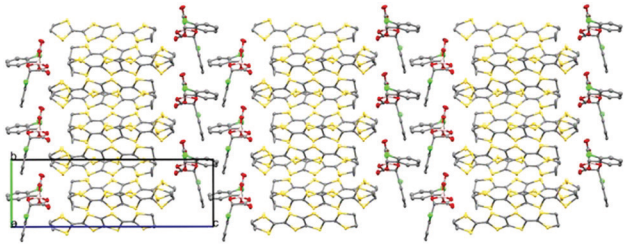

Fig. 4 Packing of **I** viewed along the *c* axis.

Due to the presence of mandelic acid moieties on the anions there are a number of hydrogen bond interactions between the anion oxygen and chlorides and the hydrogen atoms on the terminal ethyl groups of the BDH-TTP. The most prominent is that between O(2) and the disordered ethyl hydrogen atoms C(9), C(9a), C(10) and C(10a) (Fig. S1 and summarised in Table S2, ESI†), as well as the adjacent donor C(19), which could be responsible for the presence of disorder on the C(9)/C(10) group where none is present elsewhere.

MOPAC calculations[15] indicate that the $[B_S(S\text{-ClMan})_2]^-$ anion has 9.97 Debye of dipole moment, which is partially cancelled by the other anion in a unit cell. The calculation using the two anions in the unit cell elucidates that 6.03 Debye of dipole moment per one anion persists. This indicates that the crystal is not only chiral but also polar.

SQUID magnetometry (Fig. S2, ESI†) shows almost temperature-independent magnetic susceptibility of 4.5×10^{-4} emu mol^{-1}, which is likely to be Pauli paramagnetism. A Curie tail is observed at the lowest temperature. The Curie–Weiss fitting indicates that 0.41% of $S = 1/2$ spins exist as impurities.

Four-probe DC transport measurements were performed on six different single crystals of **I** which showed metallic behaviour from room temperature down to 4.2 K (Fig. 6) with a room temperature conductivity of 9.7 S cm^{-1}.

We calculated the band structure for **I** (Fig. 7) using a tight binding band structure calculation package on the basis of

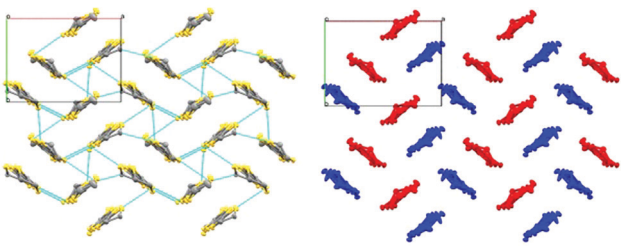

Fig. 5 κ-Type packing, with short contacts shown as blue dashed lines (left) and the crystallographically independent donors shown in red and blue (right). Thermal ellipsoids set at 50% probability, hydrogen atoms and minor disordered components omitted for clarity.

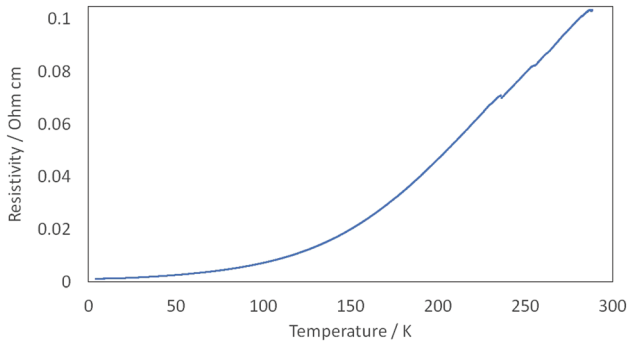

Fig. 6 Resistivity of **I**.

extended Hückel method written by Prof. Takehiko Mori.[16a,b] The figure of the band dispersions has a clear mid-gap, so called Mott gap, the width of which is 45 meV. This indicates that the band can be regarded as an effective half-filled band. The Fermi surfaces consist of hole pockets and quasi-1D sheets. If the overlap integrals in the κ-type donor layer are isotropic, the hole pockets and electron sheets gather to form a circle, at which no energy gaps between hole pockets and electron sheets are observed. **I** has a gap, 12.6% of the length of the b^* axis, which is the largest in all κ-type BDH-TTP salts whose band structures have already been reported ($[FeNO(CN)_5]PhNO_2$ salt[17] has 9.4% of gap and the other salts[18] have no gaps), suggesting that **I** has the most anisotropic Fermi surfaces of all κ-type BDH-TTP salts where the interaction along $a + b$ (n) axis is stronger than that along the $b - a$ axis. This is perhaps because **I** has the largest counter-anion. In addition, a frustration parameter t/t' of 1.24 is calculated.[19]

We report the first example of a chiral BDH-TTP radical-cation salt. This salt is a chiral metal down to 4.2 K, the lowest temperature at which metallic behaviour has been observed for a chiral molecular radical-cation salt. Work is underway to prepare the opposite enantiomer and the racemate to enable a comparison of their conducting properties. There are very few examples of chiral metals[20] available for the study of eMChA and the discovery of the first chiral molecular superconductor still proves illusive.[21] This salt has the potential to become superconducting under negative chemical pressure using a larger halogen instead of the Cl of chloromandelate. Future work will also involve synthesis of related chiral spiroboronate salts using the pool of available ligands and performing calculations on anionic diastereomers to evaluate their relative stability to further investigate the preferential crystallisation of one enantiomeric form over the other.[14]

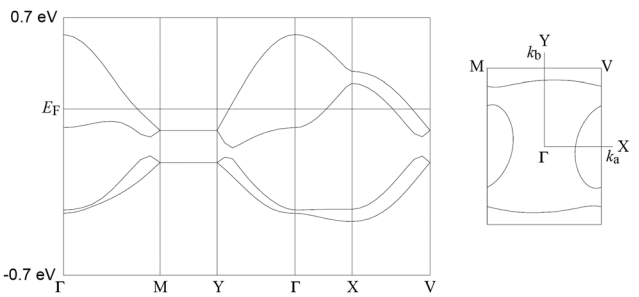

Fig. 7 Band calculation for **I** at 150 K. Transfer integrals are shown in Fig. S3 (ESI†).

L. M. and T. B. would like to thank the Royal Society and Leverhulme Trust for financial support (RPG-2019-242).

Conflicts of interest

There are no conflicts to declare.

Notes and references

‡ S-2-chloromandelic acid (0.94 g, 5 mmol) was added to a solution of boric acid (0.16 mg, 2.5 mmol) and triethylamine (2 mL, 10 mmol) in toluene (50 mL) and heated to reflux for 4 hours. The supernatant was removed *in vacuo* resulting in a clear pale yellow oil of $[NEt_3H][B(2\text{-chloromandelate})_2]$ which was used without further purification. BDH-TTP was obtained from Prof. Jun-ichi Yamada's Functional Materials II lab in University of Hyogo.[12] A mixture of BDH-TTP (10 mg, 26 μmol) and $B_{R/S}(S\text{-ClMan})_2$ (100 mg, 260 μmol) in chlorobenzene (10 mL) was filtered into a H-shaped electrochemical cell (Fig. S4). Platinum electrodes were inserted and a current of 0.5 μA was passed through the solution for a period of 18 days at room temperature resulting in dark black plates of κ-BDH-TTP$_2$[B_S-(S-ClMan)$_2$] **I**. Crystal data at 150 K: $C_{36}H_{26}BO_6S_{16}Cl_2$, M = 1149.24, black plate, a = 11.0733(7), b = 8.0039(4), c = 24.5775(11) Å, β = 99.546(5)°, U = 2148.1(2) Å^3, T = 150.00(10) K, space group $P2_1$, Z = 2, μ = 0.978 mm^{-1}, Flack parameter = −0.01(5), reflections collected = 13 309, independent reflections = 8751, $R1$ = 0.0412, w$R2$ = 0.0861 [$F^2 > 2\sigma(F^2)$], $R1$ = 0.0485, w$R2$ = 0.0901 (all data). CCDC 2069593.

1 G. L. J. A. Rikken, J. Fölling and P. Wyder, *Phys. Rev. Lett.*, 2001, **87**, 236602.
2 V. Krstic, S. Roth, M. Burghard, K. Kern and G. L. J. A. Rikken, *J. Chem. Phys.*, 2002, **117**, 11315–11319; V. Krstić and G. L. J. A. Rikken, *Chem. Phys. Lett.*, 2002, **364**, 51–56.
3 F. Qin, W. Shi, T. Ideue, M. Yoshida, A. Zak, R. Tenne, T. Kikitsu, D. Inoue, D. Hashizume and Y. Iwasa, *Nat. Commun.*, 2017, **8**, 14465; R. Wakatsuki, Y. Saito, S. Hoshino, Y. M. Itahashi, T. Ideue, M. Ezawa, Y. Iwasa and N. Nagaosa, *Sci. Adv.*, 2017, **3**, e1602390.
4 N. Avarvari and J. D. Wallis, *J. Mater. Chem.*, 2009, **19**, 4061–4076; F. Pop, N. Zigon and N. Avarvari, *Chem. Rev.*, 2019, **119**, 8435–8478.
5 F. Pop, P. Auban-Senzier, E. Canadell, G. L. J. A. Rikken and N. Avarvari, *Nat. Commun.*, 2014, **5**, 3757.
6 S. Yang, F. Pop, C. Melan, A. C. Brooks, L. Martin, P. Horton, P. Auban-Senzier, G. L. J. A. Rikken, N. Avarvari and J. D. Wallis, *CrystEngComm*, 2014, **16**, 3906–3916.
7 E. Coronado, J. R. Galán-Mascarós, C. J. Gómez-García, A. Murcia-Martinez and E. Canadell, *Inorg. Chem.*, 2004, **43**, 8072; M. Clemente-León, E. Coronado, C. J. Gómez-García, A. Soriano-Portillo, S. Constant, R. Frantz and J. Lacour, *Inorg. Chim. Acta*, 2007, **360**, 955.
8 L. Martin, H. Akutsu, P. N. Horton, M. B. Hursthouse, R. W. Harrington and W. Clegg, *Eur. J. Inorg. Chem.*, 2015, 1865; L. Martin, H. Akutsu, P. N. Horton and M. B. Hursthouse, *CrystEngComm*, 2015, **17**, 2783.
9 J. R. Lopez, L. Martin, J. D. Wallis, H. Akutsu, Y. Nakazawa, J. I. Yamada, T. Kadoya, S. J. Coles and C. Wilson, *Dalton Trans.*, 2016, **45**, 9285–9293.
10 N. Mroweh, F. Pop, C. Mézière, M. Allain, P. Auban-Senzier, N. Vanthuyne, P. Alemany, E. Canadell and N. Avarvari, *Cryst. Growth Des.*, 2020, **20**, 2516–2526; N. Mroweh, P. Auban-Senzier, N. Vanthuyne, E. Canadell and N. Avarvari, *J. Mater. Chem. C*, 2019, **7**, 12664–12673; F. Pop, P. Auban-Senzier, E. Canadell and N. Avarvari, *Chem. Commun.*, 2016, **52**, 12438–12441.
11 S. Yang, A. C. Brooks, L. Martin, P. Day, M. Pilkington, W. Clegg, R. W. Harrington, L. Russo and J. D. Wallis, *Tetrahedron*, 2010, **66**, 6977–6989.
12 J. R. Galán-Mascarós, E. Coronado, P. A. Goddard, J. Singleton, A. I. Coldea, J. D. Wallis, S. J. Coles and A. Alberolá, *J. Am. Chem.*

Soc., 2010, **132**, 9271–9273; F. Pop, S. Laroussi, T. Cauchy, C. J. Gomez-Garcia, J. D. Wallis and N. Avarvari, *Chirality*, 2013, **25**, 466–474.

13 J.-I. Yamada, H. Akutsu, H. Nishikawa and K. Kikuchi, *Chem. Rev.*, 2004, **104**, 5057–5083; A. A. Bardin, H. Akutsu and J.-i. Yamada, *Cryst. Growth Des.*, 2016, **16**, 1228–1246.

14 L. W.-Y. Wong, J. W.-H. Kan, T.-h. Nguyen, H. H.-Y. Sung, D. Li, A. S.-F. Au-Yeung, R. Sharma, Z. Lin and I. D. Williams, *Chem. Commun.*, 2015, **51**, 15760–15763.

15 J. J. P. Stewart, *MOPAC Stewart Computational Chemistry*, Colorado Springs, CO, USA, 2016, HTTP://OpenMOPAC.net/https://winmostar.com/en/.

16 (*a*) T. Mori, *Bull. Chem. Soc. Jpn.*, 1998, **71**, 2509–2526; (*b*) Program Library of Energy Band Calculation for Molecular Conductors, Takehiko Mori, Tokyo Institute of Technology, Japan, http://www.op.titech.ac.jp/lab/mori/lib/program.html.

17 I. Shevyakova, L. Buravov, V. Tkacheva, L. Zorina, S. Khasanov, S. Simonov, J. Yamada, E. Canadell, R. Shibaeva and E. Yagubskii, *Adv. Funct. Mater.*, 2004, **14**, 660–668.

18 K. Sugii, K. Takai, S. Uji, T. Terashima, H. Akutsu, A. Wada, S. Ichikawa, J. I. Yamada, T. Mori and T. Enoki, *J. Phys. Soc. Jpn.*, 2013, **82**, 054706; N. D. Kushch, A. V. Kazakova, L. I. Buravov, E. B. Yagubskii, S. V. Simonov, L. V. Zorina, S. S. Khasanov, R. P. Shibaeva, E. Canadell, H. Son and J. Yamada, *Synth. Met.*, 2005, **155**, 588–594.

19 M. Tamura, H. Tajima, K. Yakushi, H. Kuroda, A. Kobayashi, R. Kato and H. Kobayashi, *J. Phys. Soc. Jpn.*, 2020, **60**, 3861.

20 J. Short, T. J. Blundell, S. Krivickas, S. Yang, J. D. Wallis, H. Akutsu, Y. Nakazawa and L. Martin, *Chem. Commun.*, 2020, **56**, 9497–9500.

21 N. Mroweh, C. Mézière, F. Pop, P. Auban-Senzeir, P. Alemany, E. Canadell and N. Avarvari, *Adv. Mater.*, 2020, **32**(36), 2002811.